

Sustained axon regeneration induced by co-deletion of PTEN and SOCS3

Fang Sun¹, Kevin K. Park², Stephane Belin¹, Dongqing Wang³, Tao Lu⁴, Gang Chen¹, Kang Zhang⁵, Cecil Yeung¹, Guoping Feng³, Bruce A. Yankner⁴ & Zhigang He¹

A formidable challenge in neural repair in the adult central nervous system (CNS) is the long distances that regenerating axons often need to travel in order to reconnect with their targets. Thus, a sustained capacity for axon regeneration is critical for achieving functional restoration. Although deletion of either phosphatase and tensin homologue (PTEN), a negative regulator of mammalian target of rapamycin (mTOR), or suppressor of cytokine signalling 3 (SOCS3), a negative regulator of Janus kinase/signal transducers and activators of transcription (JAK/STAT) pathway, in adult retinal ganglion cells (RGCs) individually promoted significant optic nerve regeneration, such regrowth tapered off around 2 weeks after the crush injury^{1,2}. Here we show that, remarkably, simultaneous deletion of both *PTEN* and *SOCS3* enables robust and sustained axon regeneration. We further show that *PTEN* and *SOCS3* regulate two independent pathways that act synergistically to promote enhanced axon regeneration. Gene expression analyses suggest that double deletion not only results in the induction of many growth-related genes, but also allows RGCs to maintain the expression of a repertoire of genes at the physiological level after injury. Our results reveal concurrent activation of mTOR and STAT3 pathways as key for sustaining long-distance axon regeneration in adult CNS, a crucial step towards functional recovery.

During development axons reach their targets first through *de novo* outgrowth in embryos, followed by 'networked growth' in which axons elongate with termini tethered to their targets. As animals increase in body size during postnatal and adolescent stages, the distance resulted from the 'networked growth' could be much longer than that travelled by the initial *de novo* growth. After injury in the adult CNS, regenerating axons need to carry out *de novo* growth over relatively vast distances to reach their targets. Thus, the robustness of axon regeneration, in terms of both speed and duration of axon regrowth, is critical for making functional reconnections in adulthood. Approaches that have been shown to promote axon regeneration in the adult CNS include reducing extracellular inhibitory activity and increasing intrinsic growth ability^{1–9}. However, the extents of axon regeneration observed in these studies are still limited. For example, our previous studies demonstrated that the injured optic nerve could undergo significant axon regeneration after conditional deletion of *PTEN* or *SOCS3* in adult RGCs, but the regrowth only occurred during the first 2 weeks after injury, and then subsided afterwards^{1,2}.

To identify a strategy for promoting sustained robust axon regeneration, we assessed the effects of deleting both *PTEN* and *SOCS3* in adult RGCs on optic nerve regeneration. Adeno-associated viruses (AAV)-Cre (AAV-GFP (green fluorescent protein) as a control) were injected into the vitreous body of *PTEN*^{f/f10}, or *SOCS3*^{f/f11}, or *PTEN*^{f/f}/*SOCS3*^{f/f} mice to delete the floxed genes 2 weeks before optic nerve injury. In addition, ciliary neurotrophic factor (CNTF) was applied intravitreally

to the *SOCS3*^{f/f} or *PTEN*^{f/f}/*SOCS3*^{f/f} mice, as this enhances axon regeneration induced by *SOCS3* deletion².

At 2 weeks after injury, we observed a significant increase in axon regeneration in the double knockout group (Supplementary Fig. 1a, b). The synergistic effects of the double deletion became even more dramatic at 4 weeks after injury (Fig. 1). At 2 mm distal to the lesion site, deletion of both genes resulted in more than tenfold increase in the number of regenerating axons compared with deletion of either gene alone (Fig. 1a, b, d). In the double mutants, more than 20% of the regenerating axons reached the region proximal to the optic chiasm (Fig. 1c, d). Among the regenerating axons passing the chiasm, some crossed the midline and projected to the contralateral side, while others remained ipsilateral. Occasionally, a few axons could be seen projecting into the opposite uninjured optic nerve (Fig. 1c). Interestingly, several regenerating axons could grow even further, reaching the optic-tract brain entry zone and in the hypothalamus, the suprachiasmatic nuclei area (Supplementary Fig. 2).

Compared with wild-type animals, all three mutant groups showed significantly increased RGC survival after injury. At 2 weeks after injury, the survival was comparable among the three mutant groups (Supplementary Fig. 1c). At 4 weeks after injury, however, the number of surviving RGCs declined in the *PTEN* or *SOCS3* single mutants, whereas the survival rate was maintained in the double mutants (Fig. 1e).

To mimic a clinically relevant situation, we examined whether a delayed deletion of *PTEN* and/or *SOCS3* still promoted sustained optic nerve regeneration. Thus, we performed intravitreal AAV-Cre injection immediately after optic nerve injury (Fig. 2). It takes at least 3–6 days for Cre-dependent reporter expression to be observed (Supplementary Fig. 3a). We thus examined RGC survival and axon regeneration 3 weeks after injury in these animals. Despite similar survivals in all groups (Supplementary Fig. 3b, c), double and single mutants showed significant differences in the extents of axon regeneration (Fig. 2). At 2 mm distal to the lesion site, up to 20-fold more regenerating axons were seen in double mutants, compared with individual single mutants. Thus, adult RGCs with concomitant deletion of *PTEN* and *SOCS3* can activate a program for sustained *de novo* axon growth after injury.

We next examined what mechanism(s) contribute to the synergy produced by concurrent deletion of *PTEN* and *SOCS3*. Although mTOR activation is likely to be a major mediator of *PTEN* deletion¹, the regeneration phenotype of *SOCS3* deletion is dependent on gp130, a shared receptor component of cytokines^{12,13}. However, multiple downstream effectors have been implicated in cytokines-gp130 signalling^{12–15}. Because of a suggested relevance to axon regeneration^{16–18}, we tested the specific involvement of the transcription factor STAT3, a major target of the JAK/STAT pathway¹⁹. Upon phosphorylation-mediated activation, STAT3 accumulates in the nucleus to initiate

¹F.M. Kirby Neurobiology Center, Children's Hospital, and Department of Neurology, Harvard Medical School, 300 Longwood Avenue, Boston, Massachusetts 02115, USA. ²Miami Project to Cure Paralysis, Department of Neurological Surgery, Miller School of Medicine, University of Miami, Miami, Florida 33136, USA. ³McGovern Institute for Brain Research, Department of Brain and Cognitive Sciences, Massachusetts Institute of Technology, Cambridge, Massachusetts 02139, USA. ⁴Department of Genetics, Harvard Medical School, Boston, Massachusetts 02115, USA. ⁵Shiley Eye Center, University of California at San Diego, La Jolla, California 92093, USA.

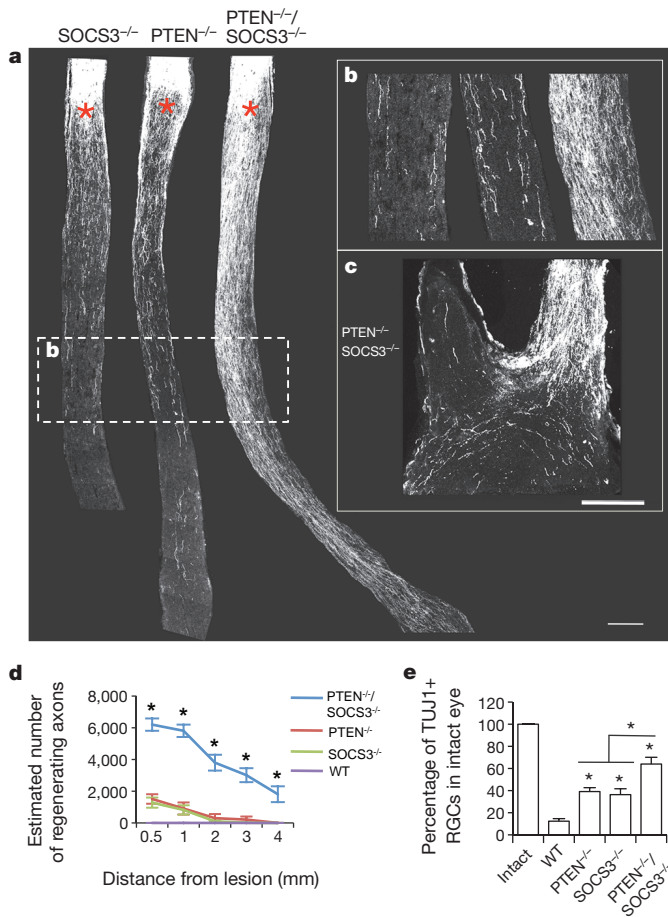


Figure 1 | Synergistic effects of double deletion of *PTEN* and *SOCS3* on axon regeneration observed at 4 weeks after injury. **a**, Images of the optic nerve sections showing CTB-labelled axons in AAV-Cre-injected *SOCS3*^{fl/fl} with CNTF (*SOCS3*^{-/-}), *PTEN*^{fl/fl} (*PTEN*^{-/-}) or *PTEN*^{fl/fl}/*SOCS3*^{fl/fl} with CNTF (*PTEN*^{-/-}/*SOCS3*^{-/-}) mice. Asterisks, lesion sites. **b**, High-magnification images of the boxed area in **a**, which is about 1.5–2.0 mm from the lesion sites. **c**, Regenerating axons at the optic chiasm. **d**, Estimated numbers of regenerating axons. There was a significant difference between the *PTEN*^{-/-}/*SOCS3*^{-/-} group and others. **P* < 0.001, ANOVA, Bonferroni's post-hoc test. **e**, Percentages of TUJ1-positive RGCs in each group compared with that in the intact retinas. **P* < 0.001, ANOVA, Tukey's post-hoc test. *N* = 7–8 per group. Error bars, s.d. Scale bars, 200 μ m.

transcription¹⁹. By immunostaining with anti-phospho-STAT3, we found that phospho-STAT3 expression was rarely detectable in intact RGCs. In wild-type mice, optic nerve injury increased phospho-STAT3 levels in RGCs, but such signals were mainly localized in the cytosol (Fig. 3a, b). In contrast, phospho-STAT3 was evident in the nuclei of axotomized RGCs with both *SOCS3* single and *SOCS3/PTEN* double mutants (Fig. 3a, b), suggesting the activation of STAT3 under these conditions.

We then evaluated the contribution of STAT3 to the axon regeneration induced by *SOCS3* deletion and CNTF administration. Deletion of *STAT3* had no significant effects on RGC survival (Supplementary Fig. 4) and axon regeneration (Fig. 3c). However, double deletion of *STAT3* and *SOCS3* abolished injury-induced phospho-STAT3 signal (Fig. 3a, b), RGC survival (Supplementary Fig. 4) and axon regeneration (Fig. 3c, d) seen in *SOCS3* single mutants, suggesting that STAT3 is a critical mediator of *SOCS3* regulated axon regeneration and RGC survival.

We next examined possible interactions of the *PTEN*- and *SOCS3*-regulated pathways on optic nerve regeneration. Similar to wild type, phospho-STAT3 expression in *PTEN*-deleted RGCs after injury was rarely detectable (Supplementary Fig. 5), arguing against STAT3

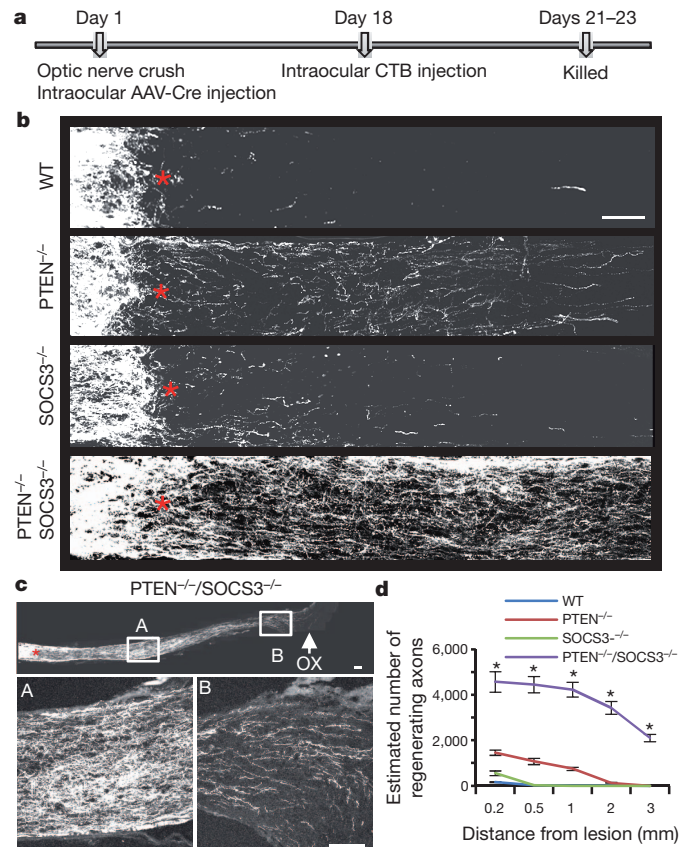


Figure 2 | Synergistic effects of double deletion of *PTEN* and *SOCS3* on optic nerve regeneration in a delayed treatment paradigm. **a**, Scheme of the experiment. **b**, Images of the optic nerve sections showing CTB-labelled axons in AAV-Cre-injected *SOCS3*^{fl/fl} with CNTF (*SOCS3*^{-/-}), *PTEN*^{fl/fl} (*PTEN*^{-/-}) or *PTEN*^{fl/fl}/*SOCS3*^{fl/fl} with CNTF (*PTEN*^{-/-}/*SOCS3*^{-/-}) mice. Asterisks, lesion sites. **c**, Extensive axon regeneration is only evident in double mutants. Top panel shows the entire optic nerve up to the chiasm. Bottom panels show high-magnified areas (**a** and **b**) as indicated in the top panel. OX, optic chiasm. **d**, Estimated numbers of regenerating axons. At all distances quantified, there was a significant difference between the *PTEN*^{-/-}/*SOCS3*^{-/-} group and the remaining groups. **P* < 0.001, ANOVA, Bonferroni's post-hoc test. *N* = 5–6 per group. Error bars, s.d. Scale bars, 100 μ m.

activation after *PTEN* deletion. Importantly, the extents of axon regeneration and RGC survival were similar in the animals with *PTEN* single deletion and *PTEN/STAT3* or *PTEN/gp130* double deletion (Fig. 4a, c and Supplementary Fig. 6a, b), suggesting that STAT3 is unlikely to be an important mediator of *PTEN* deletion.

We also evaluated the potential role of mTOR activation in axon regeneration induced by *SOCS3* deletion. Although systematic administration of rapamycin, a specific mTOR inhibitor, abolished most of the axon regeneration after *PTEN* deletion (Fig. 4a, c), the same treatment did not affect axon regeneration from *SOCS3*-deleted RGCs (Fig. 4b, d). These results suggest that these two pathways act independently in regulating axon regeneration.

To assess possible gene expression alteration triggered by *PTEN/SOCS3* double-deletion, we performed gene-expression profiling studies. Transgenic YFP17 mice expressing yellow fluorescent protein (YFP) in most RGCs (with only few amacrine cells, Supplementary Fig. 7a), either in a control background or crossed to three different mutants, were subjected to AAV-Cre injection and optic nerve injury. Three days after injury, RNA was extracted from fluorescence-activated cell sorted (FACS) RGCs for microarray analysis (Supplementary Fig. 7b–e).

The first potential mechanism is that certain key regeneration-promoting genes are significantly altered by *PTEN/SOCS3* double deletion, when compared with both single deletions and the wild-type

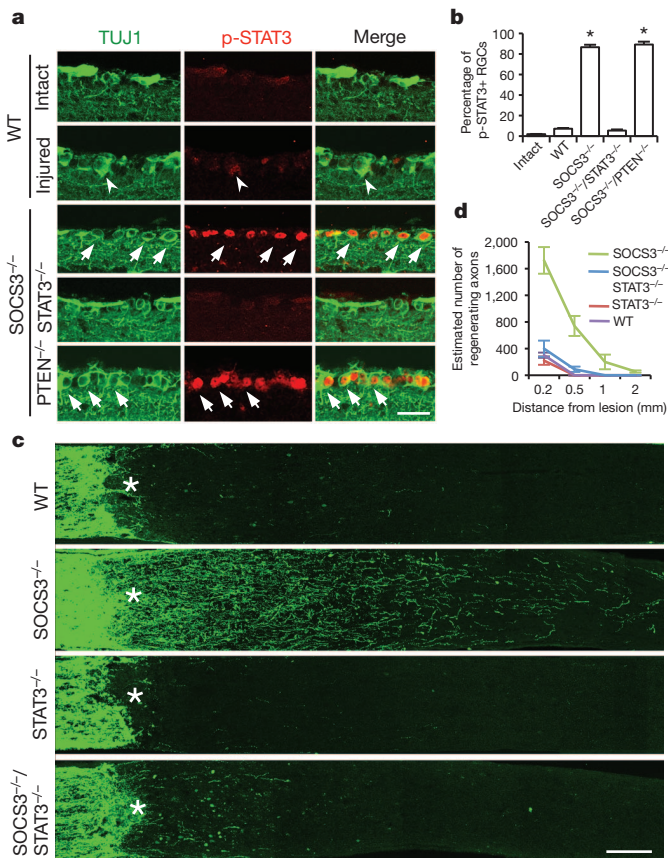


Figure 3 | Activation of STAT3 in axon regeneration induced by *SOCS3* deletion. **a**, Images showing signals detected with TUJ1 or anti-p-STAT3 antibodies in the retinal sections from intact mice or those 1 day after injury. **b**, Percentage of RGCs with nuclear phospho-STAT3 signals. $N = 3-4$ per group. $*P < 0.001$, ANOVA, Dunnett's post-hoc test. **c**, **d**, Images (**c**) and quantification (**d**) of optic nerve sections showing regenerating axons in each group at 14 days after injury. By Bonferroni's post-hoc test, regenerating axons in *SOCS3*^{-/-}/*STAT3*^{-/-} double mutants were significantly less than those in the *SOCS3*^{-/-} mutants at 0.2–2.0 mm from the lesion site ($P < 0.01$; $N = 5$ per group). Error bars, s.d. Scale bars, 50 μm in (**a**), 100 μm in (**c**).

controls. Among 15 genes selected, two encode critical positive mTOR regulators, namely small GTPase Rheb and insulin-like growth factor 1 (IGF1)²⁰ (Supplementary Figs 8 and 11), suggesting that positive feedback regulation of the mTOR activity in the double mutant may contribute to the enhanced and sustained axon regeneration. The list also includes several axon-growth-related genes, such as for the RNA-binding protein *Elavl4* (HuD), the cell adhesion molecules MAM domain-containing glycosylphosphatidylinositol anchor 2 (*Mdga2*)²¹, procadherin beta 9 (*Pcdhb9*)²², the axon guidance molecule *Unc5D*²³ and a cAMP-regulator phosphodiesterase 7B (*Pde7b*)²⁴ (Supplementary Figs 8 and 11).

In addition, double deletion may 'enhance' the regeneration-related gene-expression changes that occur poorly or moderately in the single mutants. By the criteria of significant changes ($q > 0.05$, fold change < 1.6) for comparisons between the double mutants and wild-type controls, but not between the single mutants and wild-type controls, we revealed the gene set shown in Supplementary Fig. 9a. This includes most of genes shown in Supplementary Fig. 8. Further, it shows the upregulation of several axon-growth-related genes, such as those for the signalling molecule mitogen-activated protein kinase kinase (*Map2k4*)²⁵ and the axon transport components dynein component *Dync1li2*, kinesin family member *Kif21a* and kinesin-associated protein 3 (*Kifap3*)^{26,27} (Supplementary Fig. 9a, 11). Consistently, pathway analysis indicates that this list is enriched in genes serving cellular functions related to axon growth (Supplementary Fig. 9b).

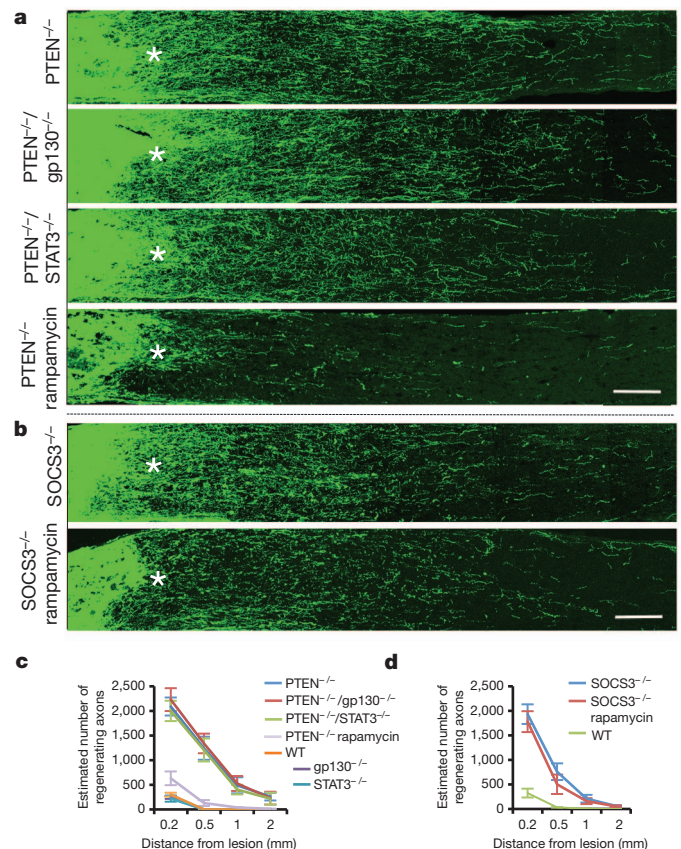


Figure 4 | Independence of PTEN- and SOCS3-regulated pathways. **a**, **b**, Images of optic nerve sections from *PTEN*^{-/-} and various *PTEN*^{-/-} combined groups (**a**) or *SOCS3*^{-/-} mutants with or without rapamycin treatment (**b**) at 14 days after injury. **c**, **d**, Quantification of regenerating axons shown in **a** and **b** respectively. **c**, Axon regeneration in either the *PTEN*^{-/-}/*gp130*^{-/-} or *PTEN*^{-/-}/*STAT3*^{-/-} group was comparable to that in *PTEN*^{-/-}, but was significantly reduced in the *PTEN*^{-/-} group with rapamycin ($P < 0.01$, ANOVA, Bonferroni's post-hoc test; $N = 5$ per group). **d**, Rapamycin treatment did not significantly reduce the number of regenerating axons in *SOCS3*^{-/-} mice ($N = 6$ per group). Error bars, s.d. Scale bars, 100 μm .

Other non-exclusive possibilities may also contribute to the synergy of the double deletion. For example, *SOCS3* deletion might regulate certain axon growth-promoting genes that are poorly regulated by *PTEN* single deletion; thus, double deletion allows the actions of both mTOR activity and these genes. We therefore screened for two sets of genes preferentially regulated by *SOCS3* or *PTEN* deletion in the double deletion induced gene alteration (Supplementary Fig. 10). These lists contain several genes related to axon regeneration, but whether any of the above genes show complementary/synergistic functions is still unknown. In addition, Krüppel-like factors *KLF4* and *KLF6* showed expression changes in opposite directions (although the changes of *KLF4* did not reach statistical significance (Supplementary Fig. 11)), consistent with proposed opposite functions of these regeneration regulators⁸.

Complementarily, we assessed the expression of a subset of genes in both intact and injured RGCs by *in situ* hybridization. When compared with the expression in intact RGCs, some genes, such as *Elavl4* and *KLF6*, were induced in the mutant(s) after injury (Supplementary Fig. 12a, b), consistent with the model of the activation of axon-growth-related genes in these mutants. However, some other genes, such as axon transport genes *Dync1li2*, *Kif21a* and *Kifap3*, and a transcription factor *ZFP40*, were maintained in the double-mutant RGCs but downregulated in both wild-type and single mutant RGCs after injury (Supplementary Fig. 12c–f). These results suggested that, in addition to inducing growth-related gene expression, the double

deletion enables injured neurons to maintain their pre-injury physiological states, which might be an important contributing mechanism for the enhanced and sustained axon regeneration.

Together, our experiments reveal an important strategy for achieving sustainable *de novo* axon regrowth in the adult CNS neurons: co-activation of specific protein translations and gene transcriptions by concomitant inactivation of PTEN and SOCS3. Notably, the mTOR activity is maintained and phospho-STAT3 levels are increased in adult peripheral sensory neurons after injury^{17,28}. Thus, the activation states of these two pathways may underlie the differential regenerative abilities of CNS and PNS neurons. However, deletion of *PTEN* and *SOCS3* is not converting the CNS neurons to a PNS-like state, because *PTEN* is similarly expressed in adult PNS neurons and *SOCS3* is increased during PNS regeneration^{17,29}. Nonetheless, enhancing mTOR activity through deletion of *PTEN* or *TSC2* also drastically increases axon re-growth in PNS neurons^{29,30}, indicating deletion of *PTEN* and *SOCS3* may make an end-run around different growth-suppressive mechanisms. Considering the formidable long distances that regenerating axons must travel in the adult after injury, the synergistic effects of two different pathways suggest a potential solution to this challenge, making the goal of functional recovery more realistic.

METHODS SUMMARY

AAV-Cre injection and optic nerve injury. Adult mice were intravitreally injected with AAV-Cre and/or CNTF to the left eyes. Optic nerve injury and quantifications were done with the methods described previously¹².

Purification of RGCs. Seventy-two hours after injury, isolated retinas were incubated in digestion solution, dissociated by gentle trituration and then filtered before FACS sorting.

RNA extraction and microarray. Isolated RNA was subjected to microarray analysis. Data were log₂ transformed at probe level, and the perfect match model-based expression values were annotated and normalized using dChip. Statistical significance of gene expression differences between groups was determined by Significance Analysis of Microarrays software. After an initial filter of very low expressed genes (average log₂ transformed value <5), a false discovery rate, or *q* value, less than 0.05 was used to generate the significant gene lists. Functional analyses were performed using the Database for Annotation, Visualization and Integrated Discovery.

Full Methods and any associated references are available in the online version of the paper at www.nature.com/nature.

Received 1 June; accepted 28 September 2011.

Published online 6 November 2011.

- Park, K. K. *et al.* Promoting axon regeneration in the adult CNS by modulation of the PTEN/mTOR pathway. *Science* **322**, 963–966 (2008).
- Smith, P. D. *et al.* SOCS3 deletion promotes optic nerve regeneration *in vivo*. *Neuron* **64**, 617–623 (2009).
- Fawcett, J. Molecular control of brain plasticity and repair. *Prog. Brain Res.* **175**, 501–509 (2009).
- Filbin, M. T. Recapitulate development to promote axonal regeneration: good or bad approach? *Phil. Trans. R. Soc. B* **361**, 1565–1574 (2006).
- Fitch, M. T. & Silver, J. CNS injury, glial scars, and inflammation: inhibitory extracellular matrices and regeneration failure. *Exp. Neurol.* **209**, 294–301 (2008).
- Hellal, F. *et al.* Microtubule stabilization reduces scarring and causes axon regeneration after spinal cord injury. *Science* **331**, 928–931 (2011).
- Leibinger, M. *et al.* Neuroprotective and axon growth-promoting effects following inflammatory stimulation on mature retinal ganglion cells in mice depend on ciliary neurotrophic factor and leukemia inhibitory factor. *J. Neurosci.* **29**, 14334–14341 (2009).
- Moore, D. L. *et al.* KLF family members regulate intrinsic axon regeneration ability. *Science* **326**, 298–301 (2009).

- Winzeler, A. M. *et al.* The lipid sulfatide is a novel myelin-associated inhibitor of CNS axon outgrowth. *J. Neurosci.* **31**, 6481–6492 (2011).
- Groszer, M. *et al.* Negative regulation of neural stem/progenitor cell proliferation by the Pten tumor suppressor gene *in vivo*. *Science* **294**, 2186–2189 (2001).
- Mori, H. *et al.* Socs3 deficiency in the brain elevates leptin sensitivity and confers resistance to diet-induced obesity. *Nature Med.* **10**, 739–743 (2004).
- Fasnacht, N. & Muller, W. Conditional gp130 deficient mouse mutants. *Semin. Cell Dev. Biol.* **19**, 379–384 (2008).
- Ernst, M. & Jenkins, B. J. Acquiring signalling specificity from the cytokine receptor gp130. *Trends Genet.* **20**, 23–32 (2004).
- Park, K. K. *et al.* Cytokine-induced SOCS expression is inhibited by cAMP analogue: impact on regeneration in injured retina. *Mol. Cell. Neurosci.* **41**, 313–324 (2009).
- Park, K., Luo, J. M., Hisheh, S., Harvey, A. R. & Cui, Q. Cellular mechanisms associated with spontaneous and ciliary neurotrophic factor-cAMP-induced survival and axonal regeneration of adult retinal ganglion cells. *J. Neurosci.* **24**, 10806–10815 (2004).
- Bareyre, F. M. *et al.* *In vivo* imaging reveals a phase-specific role of STAT3 during central and peripheral nervous system axon regeneration. *Proc. Natl Acad. Sci. USA* **108**, 6282–6287 (2011).
- Miao, T. *et al.* Suppressor of cytokine signaling-3 suppresses the ability of activated signal transducer and activator of transcription-3 to stimulate neurite growth in rat primary sensory neurons. *J. Neurosci.* **26**, 9512–9519 (2006).
- Qiu, J., Cafferty, W. B., McMahon, S. B. & Thompson, S. W. Conditioning injury-induced spinal axon regeneration requires signal transducer and activator of transcription 3 activation. *J. Neurosci.* **25**, 1645–1653 (2005).
- Aaronson, D. S. & Horvath, C. M. A road map for those who don't know JAK-STAT. *Science* **296**, 1653–1655 (2002).
- Sengupta, S., Peterson, T. R. & Sabatini, D. M. Regulation of the mTOR complex 1 pathway by nutrients, growth factors, and stress. *Mol. Cell* **40**, 310–322 (2010).
- Joset, P. *et al.* Rostral growth of commissural axons requires the cell adhesion molecule MDGA2. *Neural Develop.* **6**, 22 (2011).
- Junghans, D., Haas, I. G. & Kemler, R. Mammalian cadherins and protocadherins: about cell death, synapses and processing. *Curr. Opin. Cell Biol.* **17**, 446–452 (2005).
- Low, K., Culbertson, M., Bradke, F., Tessier-Lavigne, M. & Tuszynski, M. H. Netrin-1 is a novel myelin-associated inhibitor to axon growth. *J. Neurosci.* **28**, 1099–1108 (2008).
- Hannila, S. S. & Filbin, M. T. The role of cyclic AMP signaling in promoting axonal regeneration after spinal cord injury. *Exp. Neurol.* **209**, 321–332 (2008).
- Nix, P., Hisamoto, N., Matsumoto, K. & Bastiani, M. Axon regeneration requires coordinate activation of p38 and JNK MAPK pathways. *Proc. Natl Acad. Sci. USA* **108**, 10738–10743 (2011).
- Hanz, S. & Fainzilber, M. Retrograde signaling in injured nerve—the axon reaction revisited. *J. Neurochem.* **99**, 13–19 (2006).
- Hoffman, P. N. A conditioning lesion induces changes in gene expression and axonal transport that enhance regeneration by increasing the intrinsic growth state of axons. *Exp. Neurol.* **223**, 11–18 (2010).
- Park, K. K., Liu, K., Hu, Y., Kanter, J. L. & He, Z. PTEN/mTOR and axon regeneration. *Exp. Neurol.* **223**, 45–50 (2010).
- Abe, N., Borson, S. H., Gambello, M. J., Wang, F. & Cavalli, V. Mammalian target of rapamycin (mTOR) activation increases axonal growth capacity of injured peripheral nerves. *J. Biol. Chem.* **285**, 28034–28043 (2010).
- Christie, K. J., Webber, C. A., Martinez, J. A., Singh, B. & Zochodne, D. W. PTEN inhibition to facilitate intrinsic regenerative outgrowth of adult peripheral axons. *J. Neurosci.* **30**, 9306–9315 (2010).

Supplementary Information is linked to the online version of the paper at www.nature.com/nature.

Acknowledgements We thank M. Curry and C. Wang for technical support, H. Sasaki and F. Wang for providing Stat3^{fl/fl} and Rosa-lox-STOP-lox-Tomato mice, J. Gray, M. Hemberg, J. Choi, J. Ngai and W. Wang for advice on microarray and data analysis, and J. Gray, X. He, T. Schwarz, F. Wang, W. Wang and C. Woolf for reading the manuscript. This study was supported by grants from Wings for Life (to F.S.), Miami Project to Cure Paralysis (to K.K.P.) and NEI (to Z.H.).

Author Contributions F.S., K.K.P., K.Z. and Z.H. conceived and F.S., K.K.P., S.B., G.C. and C.Y. performed the experiments. D.W. and G.F. provided YFP-17 mice, F.S., T.L., B.A.Y. and Z.H. analysed gene array data. F.S., K.K.P. and Z.H. prepared the manuscript.

Author Information Microarray data are deposited in Gene Expression Omnibus under accession number GSE32309. Reprints and permissions information is available at www.nature.com/reprints. The authors declare competing financial interests: details accompany the full-text HTML version of the paper at www.nature.com/nature. Readers are welcome to comment on the online version of this article at www.nature.com/nature. Correspondence and requests for materials should be addressed to Z.H. (Zhigang.he@childrens.harvard.edu).

METHODS

AAV-Cre injection. All experimental procedures were performed in compliance with animal protocols approved by the Institutional Animal Care and Use Committee at Children's Hospital, Boston. C57BL6/J mice (WT) or various floxed mice including Rosa-lox-STOP-lox-Tomato (from F. Wang), *SOCS3^{fl/fl}*, *PTEN^{fl/fl}*, *SOCS3^{fl/fl}/PTEN^{fl/fl}*, *STAT3^{fl/fl}*, *gp130^{fl/fl}*, *SOCS3^{fl/fl}/STAT3^{fl/fl}*, *PTEN^{fl/fl}/STAT3^{fl/fl}*, *PTEN^{fl/fl}/gp130^{fl/fl}*, YFP-17 crossed with or without *SOCS3^{fl/fl}* and/or *PTEN^{fl/fl}* were intravitreally injected with 1–2 μ l volume of AAV-Cre (titres at 0.5×10^{12} to 1.0×10^{12}) to the left eyes. For each intravitreal injection, a glass micropipette was inserted into the peripheral retina, just behind the ora serrata, and was deliberately angled to avoid damage to the lens. In some experiments, 1 μ l ($1 \mu\text{g } \mu\text{l}^{-1}$) CNTF (Pepro Tech) was intravitreally injected immediately after injury and at 3 days after injury, and weekly thereafter.

Optic nerve injury. Two weeks after AAV-Cre injection, the left optic nerve was exposed intraorbitally and crushed with jeweler's forceps (Dumont number 5; Roboz) for 5 s approximately 1 mm behind the optic disc. Counting TUJ1+RGCs in retina wholemount and regenerating axons was done with the methods described previously^{1,2}.

Purification of RGCs. YFP17 mice, either themselves or crossed with *PTEN* and/or *SOCS3* floxed mice, were subjected to AAV-Cre injection and optic nerve injury. Seventy-two hours after injury, animals were killed and retinas were immediately dissected out for dissociation. Retinas were incubated in digestion solution (20 U ml⁻¹ papain, Worthington; 1 mM L-cysteine HCL; 0.004% DNase; 0.5 mM EDTA in Neurobasal) for 30 min at 37 °C, and then moved into Ovomuroid/BSA (1 mg ml⁻¹) solution to stop digestion. Subsequently, retinas were dissociated by gentle trituration with trituration buffer (0.5% B27; 0.004% DNase; 0.5 mM EDTA in Opti-MEM), and then filtered through 40- μ m cell strainer (BD Falcon) before FACS.

FACS was performed with BD FACSAria IIu. Each time immediately before sorting, a purity test was performed to ensure the specificity for sorting YFP signal was higher than 99%. Dissociated retinal cells were separated based on both size (forward scatter) and surface characteristics (side scatter). Aggregated cells were excluded based on FSC-H:FSC-A ratio. Retinal cells without YFP expression were used as negative controls to set up the detection gate each time before sorting the YFP-positive cells. Sorted cells were immediately subjected to RNA extraction.

RNA extraction and microarray. RNA was extracted using the Qiagen RNeasy mini kit (Qiagen), and RNA quality was assessed using a bioanalyser (Agilent Technologies). For microarray assays, RNA was amplified and labelled with the NuGEN Ovation WTA System (NuGEN), to obtain 2.8 μ g of antisense RNA to be hybridized on Affymetrix mouse Genechip 1.0 ST (Affymetrix). To ensure reproducibility and biological significance, three hybridizations were performed for each group, with RNA samples collected from three independent FACS purifications, each including three or four animals (biological replicates).

Data from microarrays were log₂ transformed at probe level, and the perfect match model-based expression values were annotated and normalized using dChip (www.dchip.org <http://www.dchip.org>). Statistical significance of gene expression differences between groups was determined by Significance Analysis of Microarrays (SAM) software (<http://www-stat.stanford.edu/~tibs/SAM>). After an initial filter of very low expressed genes (average log₂ transformed value <5), a false discovery rate, or *q* value, less than 0.05 was used to generate the significant gene lists.

Functional annotation clustering analysis was performed using the Database for Annotation, Visualization and Integrated Discovery (DAVID; <http://david.abcc.ncifcrf.gov>). The functional annotation groups with similar EASE score (Fisher's exact probability value) were clustered and grouped under the same overall enrichment score. The higher the score, the more enriched. The five top-scored clusters were listed, and the count of genes and their percentage to corresponding categories in the database were shown.